# Reciprocity between Charge Injection and Extraction and Its Influence on the Interpretation of Electroluminescence Spectra in Organic Solar Cells

Thomas Kirchartz,[1,2,*] Jenny Nelson,[3] and Uwe Rau[1]

[1]*IEK5-Photovoltaik, Forschungszentrum Jülich, 52425 Jülich, Germany*
[2]*Faculty of Engineering and CENIDE, University of Duisburg-Essen, Carl-Benz-Strasse 199, 47057 Duisburg, Germany*
[3]*Department of Physics and Centre for Plastic Electronics, Imperial College London, South Kensington Campus SW7 2AZ, London, United Kingdom*

(Received 1 September 2015; revised manuscript received 5 April 2016; published 3 May 2016)

Reciprocity relations based on the principle of detailed balance have been frequently used to analyze luminescence intensity and the spectrum of organic solar cells. These reciprocity relations were derived for cases where a linear extrapolation of equilibrium conditions to the nonequilibrium situations present during measurements is possible and therefore requires semiconductors with linear recombination mechanisms. Here, we discuss the impact of nonlinear recombination typically found in organic solar cells on the analysis of luminescence spectra and estimate criteria under which reciprocity relations can still be used to analyze the data. We find that depending on the exact application, only for low mobilities $\mu < 10^{-4}\,\mathrm{cm^2/V\,s}$ or very asymmetric mobilities do substantial disagreements between simulation and analytical equations occur.

DOI: 10.1103/PhysRevApplied.5.054003

## I. INTRODUCTION

Within the last years, electroluminescence (EL) spectroscopy [1–9] and imaging of organic solar cells [10,11] have been used more and more frequently to address a variety of questions ranging from applied ones like the determination of sheet resistances [12–14], degradation behavior [15], or optimum microstructure [16] to fundamental questions like the relevance of hot charge transfer states for photocurrent generation in organic solar cells [17]. The analysis of the spectral shape and intensity of EL measurements has often [2,18–21] been performed using two reciprocity relations that relate the emission of a diode to its photovoltaic properties [22,23]. These reciprocity relations are based on the principle of detailed balance [24,25] and extrapolate the situation at thermal equilibrium to nonequilibrium situations present during EL measurements or during typical photovoltaic measurements. While the principle of detailed balance [26] is universal, its application to nonequilibrium situations is possible only if the system—in this case the solar cell—is linear in charge density. In practice, this implies that the reciprocity relations hold if the emission originates from band-to-band transitions and if the recombination mechanism is linear in minority carrier concentration. This is very often not the case in thin-film solar cells for two distinct reasons. One reason is the disordered nature of many materials used for thin-film solar cells that might lead to emission from band tails leading to nonlinear effects [27,28]. The second reason is that many solar cells (both thin-film devices and others) are fully or nearly fully depleted systems, where the space-charge region has a similar size to the whole absorber [29]. In this case, recombination becomes nonlinear because it always involves an electron and a hole, both of which change their concentration with illumination and applied bias [30–32]. Thus, in systems where the superposition principle [33] breaks down, the reciprocity relations will not be strictly valid anymore [34].

Previously, we have discussed the impact of disorder and band tails on the description of EL emission spectra [28]. However, the impact of nonlinear recombination in mostly depleted [35] solar cells has not yet been discussed in detail. Here, we employ numerical device simulations to estimate the effect of nonlinear recombination and space-charge effects on two different analysis methods that have been used in the literature. These two methods are based on (i) the correlation between the EL intensity and the open-circuit voltage of a solar cell [2,36,37] and (ii) the use of EL spectroscopy to prove the absence of the controversially discussed hot-carrier effects [38–45] in the charge separation process of organic bulk-heterojunction solar cells [17].

The first one of the previously mentioned reciprocity relations between light-emitting and photovoltaic properties links the external photovoltaic quantum efficiency $Q_e$ to the EL (excess) emission flux $\delta\phi_{\mathrm{em}}$ via [22]

$$\delta\phi_{\mathrm{em}}(E) = Q_e(E)\phi_{\mathrm{BB}}(T,E)\left[\exp\left(\frac{qV}{kT}\right) - 1\right]. \qquad (1)$$

*To whom all correspondence should be addressed.
t.kirchartz@fz-juelich.de

 

Excess flux means here the flux in excess of the flux emitted if the device is in thermal equilibrium with its environment. Thus, $\delta\phi_{\mathrm{em}}$ will be zero if the internal voltage $V$ is zero. The black body (BB) spectrum $\phi_{\mathrm{BB}}$ (units, $\mathrm{cm}^{-2}\,\mathrm{s}^{-1}\,\mathrm{eV}^{-1}$) is given by

$$\phi_{\mathrm{BB}}(T,E) = \frac{2\pi E^2}{h^3c^2}\frac{1}{[\exp(E/kT)-1]} \approx \frac{2\pi E^2}{h^3c^2}\exp\left(\frac{-E}{kT}\right), \tag{2}$$

and mainly depends on the temperature $T$ of the solar cell and on the photon energy $E$. In addition, $k$ is the Boltzmann constant, $q$ the elementary charge, and $V$ the internal voltage, defined as the quasi-Fermi-level splitting at the edge of the space-charge region (see Ref. [28] for a discussion on the definition of the internal voltage).

While Eq. (1) defines the spectral shape of the EL spectrum, it is also possible to relate the intensity of the EL emission to the open-circuit voltage of a solar cell [46]. The only unavoidable recombination mechanism in a solar cell is radiative recombination. Therefore, the situation with the highest open-circuit voltage (smallest recombination at given carrier concentrations) will be the so-called radiative limit. In the radiative limit, the LED quantum efficiency

$$Q_{\mathrm{LED}} = \frac{J_{\mathrm{em}}}{J_{\mathrm{ne}} + J_{\mathrm{em}}}, \tag{3}$$

of a device will be one, where $J_{\mathrm{em}}$ is the current density leading to photon emission and $J_{\mathrm{ne}}$ the current density not leading to photon emission which would be zero in the radiative limit. Introducing nonradiative recombination will at the same time reduce the open-circuit (OC) voltage relative to its upper limit—the radiative open-circuit voltage $V_{\mathrm{OC,rad}}$—and it will reduce the LED quantum efficiency (because of the increase in $J_{\mathrm{ne}}$). Therefore, it is intuitively clear that there should be a relation between the difference $V_{\mathrm{OC,rad}} - V_{\mathrm{OC}}$ and the LED quantum efficiency $Q_{\mathrm{LED}}$. It can be shown that such a relation exists and reads [22] (see also Refs. [46,47] for earlier versions)

$$V_{\mathrm{OC,rad}} - V_{\mathrm{OC}} = -\frac{kT}{q}\ln(Q_{\mathrm{LED}}). \tag{4}$$

Because of Eq. (1), the radiative open-circuit voltage can be written and determined via

$$V_{\mathrm{OC,rad}} = \frac{kT}{q}\ln\left(\frac{q\int_0^\infty Q_e\phi_{\mathrm{sun}}dE}{q\int_0^\infty Q_e\phi_{\mathrm{BB}}(T)dE} + 1\right) \tag{5}$$

if Eq. (1) is valid. Here, $\phi_{\mathrm{sun}}$ is the spectrum of solar radiation (typically AM1.5G). Equation (4) implies that for each decade of loss in $Q_{\mathrm{LED}}$, the $V_{\mathrm{OC}}$ should be reduced by $kT\ln(10) \approx 58$ meV.

## II. PREDICTION OF $V_{\mathrm{OC}}$ FROM EL INTENSITY

Equations (1) and (4) rely on the validity of the so-called Donolato theorem [24,48–51] that connects injection and extraction under certain conditions. Figure 1 visualizes the situation to which the Donolato theorem applies. The typical situation encountered in many solar cells is, e.g., a $p$-type material that forms a $p$-$n$ junction or Schottky junction at one side with a space-charge region that is small compared to the total absorber thickness as shown in Fig. 1(a). In the base of this device, there is nearly no electric field and drift of minority carriers is negligible. Charge collection depends on the diffusion length and the distance to the collecting junction. The collection efficiency $f_c(x)$ for electrons in a $p$-type semiconductor will decrease as a function of distance from the junction as shown in Fig. 1(b). In this case, i.e., assuming a field-free doped-base region of a $p$-$n$ junction or Schottky junction, the Donolato theorem [48–52] specifies that

$$f_c(x) = \frac{\Delta n(x)}{n_0[\exp(\frac{qV}{kT}) - 1]}, \tag{6}$$

and thereby connects the collection efficiency under illumination at short circuit with the injection of charge

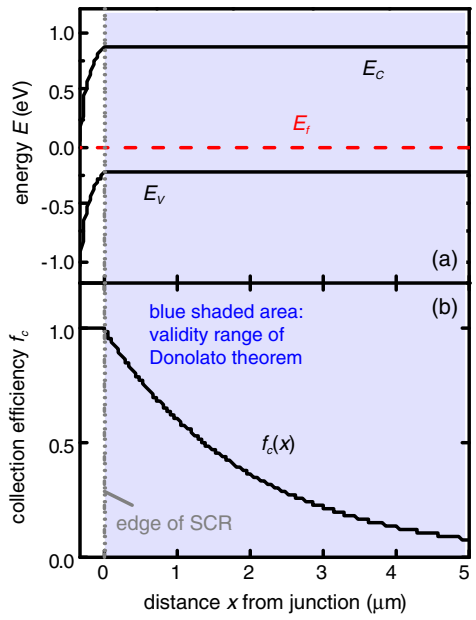


FIG. 1. (a) Band diagram of a solar cell with a large neutral region and a small space-charge region at zero applied bias in the dark. In the neutral region (blue shaded area) of such a device as depicted in (a), the collection efficiency [shown in (b)] for minority carriers (here electrons) decays towards the back contact. The exact shape of the decay of the collection efficiency at short circuit under illumination will depend on the bulk diffusion length and the surface recombination velocity and it will be identical to the normalized minority carrier concentration in the dark (Donolato theorem).

carriers under forward bias in the dark which would be relevant, e.g., to describe luminescence emission. Here, $n_0$ is the equilibrium concentration of electrons and $\Delta n$ is the excess electron concentration. Equation (6) implies that the collection efficiency is identical to the excess electron concentration $\Delta n(x)$ normalized to the excess electron concentration at the edge of a space-charge region (of course, an analogous version of Eq. (6) can be defined for holes in an $n$-type semiconductor). The Donolato theorem describes only the relation between collection and injection in a semiconductor in low-level injection. In the case of a $p$-type semiconductor, that means that the electron concentration is always much smaller than the hole concentration. The condition of low-level injection is typically valid in the neutral base of a $p$-$n$ diode but not in its space charge region nor in the intrinsic region of a $p$-$i$-$n$-diode or a metal-insulator-metal-type device structure. Thus, if a large fraction of the photovoltaically active layer consists of a depletion region, both carrier concentrations will be a function of voltage and illumination and recombination will be nonlinear. In these cases, the Donolato theorem cannot be derived anymore. However, it is possible to estimate the impact of the violation of the Donolato theorem on the calculation of $V_{\mathrm{OC,rad}}$ and on the estimation of the open-circuit voltage loss [21,53–55] $\Delta V_{\mathrm{OC}} = V_{\mathrm{OC,rad}} - V_{\mathrm{OC}}$ due to nonradiative recombination using the LED quantum efficiency $Q_{\mathrm{LED}}$ via $\Delta V_{\mathrm{OC}} = -kT/q \ln(Q_{\mathrm{LED}})$.

The Donolato theorem specifies that the spatial profile of injected minority carriers and of the probability for minority carrier collection are identical. The shape and intensity of the EL spectrum depends not only on how many photons are generated in the volume of the device, but also on how likely it is they will leave the device and not be reabsorbed. In crystalline Si solar cells, the spatial profile of minority carriers injected at one contact leads to an energy dependence of the EL emission because of reabsorption effects [22,56,57]. The closer a photon is emitted to the front contact and the lower its energy, the less likely it will be reabsorbed. In organic solar cells, however, the active layer is about 3 orders of magnitude thinner than in typical $c$-Si solar cells and the quantum efficiency at the emission peak is typically 6 to 7 orders of magnitude lower than the peak of the quantum efficiency [17,58–61]. In consequence, reabsorption effects would be expected to be small and often negligible in thin devices. However, in organic solar cells the active layer thickness is on the order of the wavelength of light, therefore interference effects would be relevant and could affect the shape of the spectrum. In the following, we will first study the effect of transport on the validity of Eq. (4). Here only the absolute value of the emission is relevant and we will neglect the effects of reabsorption or interference. In the second part of the manuscript, the shape of the EL spectrum and the validity of Eq. (1) will be discussed and therefore interference effects are taken into account.

The prediction of $V_{\mathrm{OC}}$ using the calculated $V_{\mathrm{OC,rad}}$ and the measured LED quantum efficiency $Q_{\mathrm{LED}}$ will be affected by the fact that recombination is nonlinear and that the collection efficiency will be voltage dependent. The latter fact is well known for the case of organic solar cells, because a voltage-dependent collection efficiency is one of the causes of a voltage-dependent corrected photocurrent as has been measured and simulated various times [62–66]. Corrected photocurrent means in this context that the photocurrent is determined by subtracting the dark current from the current under illumination for each voltage. The prediction of $V_{\mathrm{OC}}$ could also be affected by luminescence being emitted from band tails or other types of localized states such that the emission $\delta\phi_{\mathrm{em}}$ would not be proportional $\exp(qV/kT)$ anymore as predicted by Eq. (1). This effect has been discussed in more detail in Ref. [28] and is neglected here. Usually it can be tested whether the proportionality $\delta\phi_{\mathrm{em}} \sim \exp(qV/kT)$ breaks down by checking whether the shape of the EL spectrum is voltage dependent. Most, but not all, organic solar cells show negligible peak shift [28].

In the following, we therefore first focus on the case that EL emission does not shift with voltage or injection current and that it can be described as a recombination between two quasifree carriers whose occupation probability approximately follows Boltzmann statistics. For this case, we show in the Supplemental Material [67] that the error between predicted $V_{\mathrm{OC,pred}} = V_{\mathrm{OC,rad}} - kT \ln(Q_{\mathrm{LED}})$ and the actual $V_{\mathrm{OC,exact}}$ is

$$V_{\mathrm{OC,pred}} - V_{\mathrm{OC,exact}} = \frac{kT}{q} \ln\left(\frac{F_i(V_{\mathrm{OC}})}{F_c(V_{\mathrm{OC}})}\right) \tag{7}$$

with the spatially averaged collection efficiency $F_c(V) = \frac{1}{d}\int_0^d f_c(x)dx$ and the spatially averaged injection efficiency that we define as

$$F_i(V) = \frac{1}{d}\int_0^d \frac{n(x,V)p(x,V) - n_i^2}{n_i^2[\exp(\frac{qV}{kT}) - 1]}dx. \tag{8}$$

Note that the spatially averaged collection efficiency $F_c(V)$ is the corrected photocurrent $J_{\mathrm{ph}}(V)$ (difference between light and dark current voltage curves) normalized to the maximum photocurrent $J_{\mathrm{phmax}} = qGd$.

In the following, we will employ drift-diffusion simulations using the software ASA [68] to simulate the influence of finite collection efficiencies on the prediction of $V_{\mathrm{OC}}$. In Figs. 2(a) and 2(b) we simulate the voltage dependence of collection and injection efficiency for a case with high mobilities, i.e., efficient collection and extraction and one case with low mobilities (see Table I for simulation parameters). In the high-mobility case [Fig. 2(a)], collection and injection efficiencies are close to one for lower voltages. Only for voltages close to $V_{\mathrm{OC}}$, both $F_i$ and $F_c$ decrease, but their values are still similar at

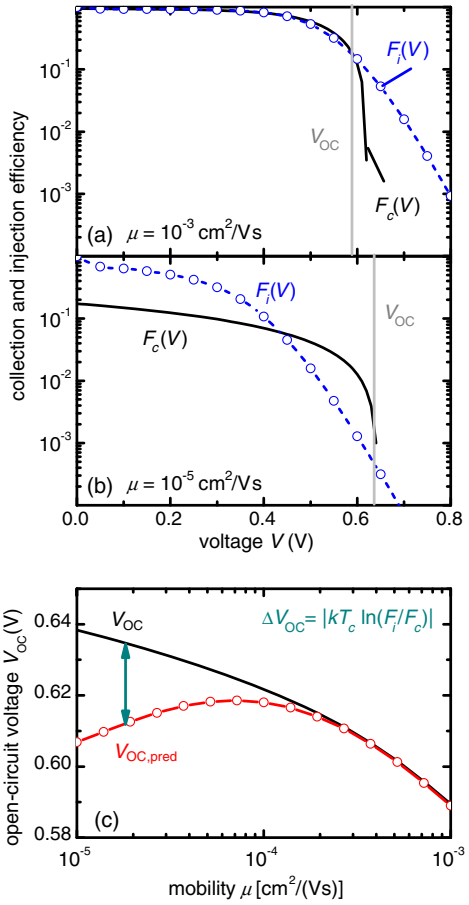


FIG. 2. (a),(b) Comparison of the voltage dependence of spatially averaged injection and extraction probabilities for two different mobilities. (c) Influence of mobility on the prediction of $V_{oc}$ using the LED quantum efficiency and Eq. (7).

$V_{OC}$ (the difference is hardly distinguishable on the log plot). In the low mobility case, the collection and injection efficiency are different already at low voltages. Here, recombination at short circuit is substantial, so collection is already reduced at short circuit, while the injection efficiency is per definition always one at short circuit. Also close to open circuit, the differences between collection and injection are larger than for the high-mobility case.

Figure 2(c) summarizes the results and shows the exact and the predicted $V_{OC}$ based on the simulations of collection and injection efficiency. In the case of reasonably high mobilities, the prediction of $V_{OC}$ using the method of Vandewal *et al.* [2] should work nearly perfectly despite the violation of the Donolato theorem. Only in cases where the cell has rather low mobilities $\mu < 10^{-4}$ cm$^2$/V s and therefore low efficiencies, the violation of the Donolato theorem leads to a substantial deviation between prediction and exact $V_{OC}$. Thus, for reasonably efficient polymer:fullerene solar cells, the prediction of $V_{OC}$ using the LED quantum efficiency should not be affected by the violation of the Donolato theorem. In order to explore a larger parameter space, additional simulations are provided in the Supplemental Material, Sec. B [70].

## III. ENERGY VS POSITION-DEPENDENT CHARGE-CARRIER COLLECTION

Recently, Vandewal *et al.* [17] used the validity of the reciprocity between electroluminescence spectrum and photovoltaic quantum efficiency [Eq. (1)] as evidence for the insensitivity of photon energy to the charge generation efficiency in bulk-heterojunction solar cells based on polymers and/or small molecules. Figure 3 illustrates the basic idea behind the approach of Ref. [17]. If the dissociation efficiency of charge transfer states is independent of energy as assumed in Fig. 3(a), the reciprocity

TABLE I. Parameters used for the simulations shown in Figs. 2 and 4. For the definition of the capture coefficients see Fig. 2 in Ref. [69].

| | | Figure 2 | Figure 4 |
|---|---|---|---|
| Band mobility | $\mu_n$ [cm$^2$/V s] | Variable | $10^{-3}$ or $10^{-4}$ |
| | $\mu_p$ [cm$^2$/V s] | Variable | $10^{-3}$ or $10^{-4}$ |
| Effective density of states | $N_C = N_V$ [cm$^{-3}$] | $10^{19}$ | $10^{19}$ |
| Density of tail states | $N_{Ctail} = N_{Vtail}$ [cm$^{-3}$] | $2.5 \times 10^{18}$ | $2.5 \times 10^{18}$ |
| Characteristic tail slope | $E_{chC} = E_{chV}$ [meV] | 50 | 50 |
| Capture coefficients | $\beta_n^+$ [cm$^3$ s$^{-1}$] | $10^{-12}$ | $10^{-12}$ |
| | $\beta_p^0$ [cm$^3$ s$^{-1}$] | $10^{-10}$ | $10^{-10}$ |
| | $\beta_p^-$ [cm$^3$ s$^{-1}$] | $10^{-12}$ | $10^{-12}$ |
| | $\beta_n^0$ [cm$^3$ s$^{-1}$] | $10^{-10}$ | $10^{-10}$ |
| Band gap | $E_g$ [eV] | 1.0 | 1.0 |
| Thickness | $d$ [nm] | 150 | 200 |
| Doping concentration | $N_A$ [cm$^{-3}$] | 0 | 0 if not stated otherwise |
| Surface recombination velocity | $S$ [cm/s] | $10^5$ | $10^5$ |
| Contact barrier heights | $\varphi_b$ [meV] | 0.15 | 0.15 |
| Generation rate | $G$ [cm$^{-3}$ s$^{-1}$] | $4 \times 10^{21}$ | Calculated with a TM algorithm |

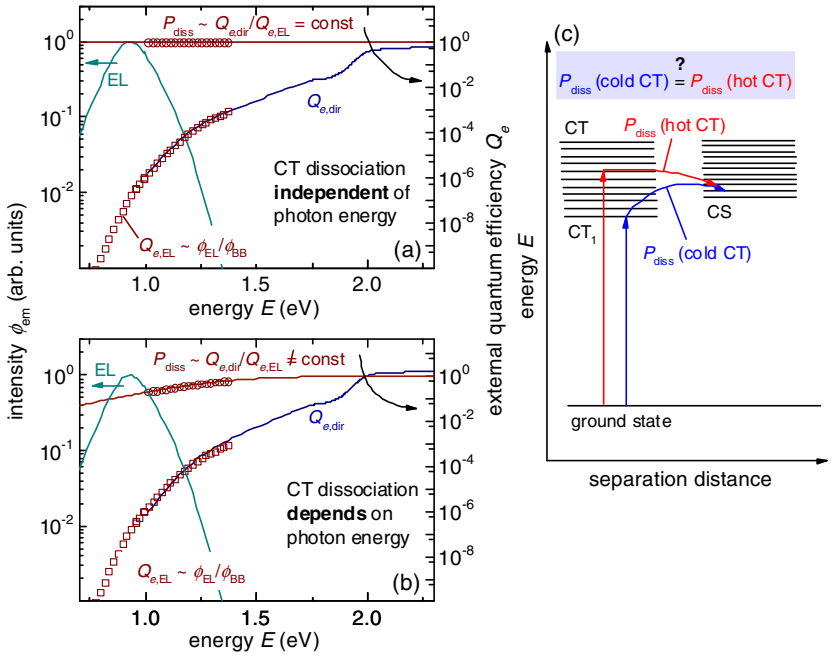


FIG. 3. Schematic graphs showing how a comparison of the direct and derived quantum efficiencies $Q_{e,\mathrm{dir}}$ and $Q_{e,\mathrm{EL}}$ have been used by Vandewal *et al.* to determine whether the dissociation probability $P_{\mathrm{diss}}$ of CT states depends on photon energy. (a) shows the case as observed in experiment, where $P_{\mathrm{diss}} = \mathrm{const}$ and (b) shows the hypothetical case where $P_{\mathrm{diss}} \neq \mathrm{const}$. (c) is a schematic energy diagram showing CT states with different energies and the CS denotes the charge separated state.

should be valid, i.e., the directly measured quantum efficiency $Q_{e,\mathrm{dir}}$ should be roughly equal to the quantum efficiency $Q_{e,\mathrm{EL}}$ determined from the EL spectrum using Eq. (1). If the dissociation efficiency is energy dependent, i.e., hot charge-transfer (CT) states are more likely to dissociate due to their excess energy than cold CT states, the situation as shown in Fig. 3(b) would be expected. In the region, where $Q_{e,\mathrm{dir}}$ and $Q_{e,\mathrm{EL}}$ overlap, they should have a different shape. The ratio $Q_{e,\mathrm{dir}}/Q_{e,\mathrm{EL}}$ should then be increasing with energy and be proportional to the dissociation efficiency of CT states. This is because the dissociation efficiency $P_{\mathrm{diss}}$ affects the generation of charges as measured in the quantum efficiency $Q_{e,\mathrm{dir}}$ while the EL would be unaffected by effects from hot CT states, because the injected charges are expected to be thermally relaxed under typical injection conditions. Studying the ratio $Q_{e,\mathrm{dir}}/Q_{e,\mathrm{EL}}$ in different donor-acceptor blends should therefore help to decide whether the dissociation of hot CT states is more efficient as that of cold CT states as schematically depicted in Fig. 3(c). The result of Vandewal *et al.* [17] is that the dissociation efficiency of CT states or the generation efficiency of charge separated states does not depend on photon energy in a relatively wide range of photon energies, therefore implying that CT states probably thermalize faster than they dissociate and that dissociation from the lowest energy CT state [$CT_1$ in Fig. 3(c)] is still efficient in efficient organic solar cells.

However, in order to correctly analyze the ratio $Q_{e,\mathrm{dir}}/Q_{e,\mathrm{EL}}$, it is useful to check whether any of the other assumptions required for Eq. (1) to hold might be violated. As discussed before, the Donolato theorem is generally not valid in systems that are mostly depleted and where recombination is therefore nonlinear and depending on electron and hole concentration instead of only depending on the minority carrier concentration. The question is, however, whether a violation of the Donolato theorem could affect the energy dependence of electroluminescence spectrum or quantum efficiency.

In general, differences between the terms for injection (in EL) and extraction (in the quantum efficiency) can lead to changes in the spectral shape if either reabsorption or interference effects are taken into account. So far, we neglected these effects and assumed that only the spatially averaged collection and injection efficiencies matter. However, even in the weak absorption limit, where the absorption coefficient ($\alpha$)-thickness ($d$) product is small ($\alpha d \ll 1$) and reabsorption is negligible, interferences can modify the probability for spontaneous emission (the Purcell effect). According to Kirchhoff's law, the emissivity and absorptance of a body are identical. Therefore, there must be a direct connection between generation rates and emission probabilities. Under the assumption that radiative recombination is proportional to the product $np$ of free electron and hole concentrations (again neglecting emission from traps or band tails), we can express the electroluminescence emission in a diode using [25]

$$\phi_{\mathrm{em}}(E,V) = \int_0^d g(x,E)\frac{n(x,V)p(x,V) - n_i^2}{n_i^2} dx \phi_{\mathrm{BB}}(E), \tag{9}$$

where $g(x,E)$ is the generation rate normalized to the incident photon flux. Note that the fact that part of the light created by radiative recombination does not leave the device but is totally internally reflected is already taken into account by the definition of $\phi_{\mathrm{BB}}$ in Eq. (2).

Again, we are using the software ASA to simulate different situations. In addition to the electrical model used previously, we also use ASA's built-in transfer matrix code GENPRO1 to take interference effects into account. To estimate the influence of interference on the reciprocity relations, we simulate the quantum efficiency directly and via Eqs. (9) and (1). Thus, we compare the two terms

$$Q_{e,\mathrm{EL}}(E,V) = \int_0^d g(x,E) f_{\mathrm{i}}(x,V) dx \tag{10a}$$

and

$$Q_{e,\mathrm{dir}}(E,V) = \int_0^d g(x,E) f_c(x) dx. \tag{10b}$$

Here, the spatially resolved injection efficiency $f_i$ is

$$f_i(x,V) = \frac{n(x,V)p(x,V) - n_i^2}{n_i^2[\exp(\frac{qV}{kT}) - 1]} \tag{11}$$

in analogy to Eq. (8), which defines the spatially averaged injection efficiency. If we compare spatially resolved collection and injection efficiency in thin devices ($d < 100$ nm), they are rather similar and small differences will be seen between $Q_{e,\mathrm{EL}}$ and $Q_{e,\mathrm{dir}}$ [71]. Larger differences can be seen for slightly larger thicknesses ($d > 200$ nm) that are typically used for some organic solar-cell materials like P3HT:PCBM and for cases where the mobilities are asymmetric and therefore create a space-charge region that is smaller than the active layer thickness.

Figure 4(a) compares the injection and extraction efficiency for a device of thickness $d = 200$ nm with asymmetric mobilities (electron mobility $\mu_n = 10\ \mu_p$, $\mu_p$: hole mobility). The collection efficiency is calculated for the situation of short circuit in the dark with additional position-dependent photogeneration with light of negligible intensity. Therefore, there are hardly any photogenerated carriers in the device and the asymmetric mobilities do not influence the electrostatics in the device much. The collection efficiency is therefore relatively symmetric and homogenous over the device thickness. At the contacts, the collection probability is reduced because we assumed the contacts to be effective recombination centers for minority carriers. We simulate the injection efficiency at a forward bias of $V = 0.8$ V, which is a representative value for the internal voltage during an electroluminescence measurement. At the forward biases needed to measure electroluminescence, the device is full of electrons and holes injected from the contact that rearrange themselves according to their different mobilities. This injected charge affects the electrostatics such that the injection efficiency is much higher towards the front contact (anode) than it is towards the back contact (cathode). Thus, we have created a situation where

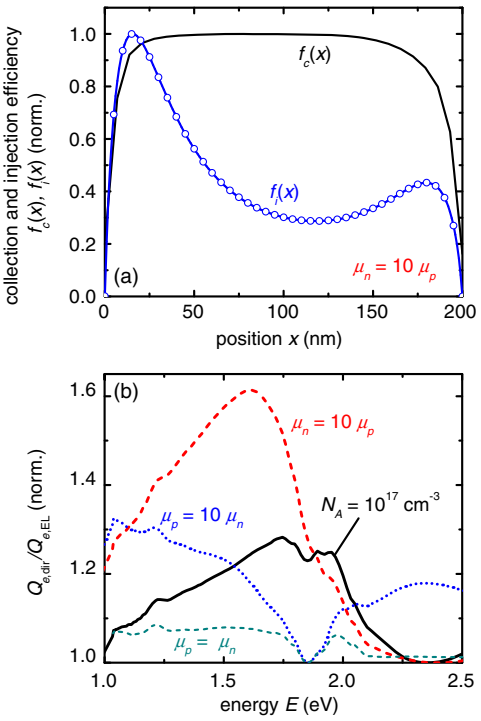


FIG. 4. (a) Comparison of spatially resolved injection (at $V = 0.8$ V) and extraction probabilities (at short circuit, no bias light). Particularly large differences happen for a material with asymmetric mobilities and higher thicknesses. (b) Ratio of direct and derived quantum efficiency for different situations (symmetric mobilities, asymmetric mobilities, and doping).

injection and extraction efficiencies have a different position dependence. This is because the extraction efficiency is simulated for a situation that is very close to equilibrium (representative of a quantum efficiency measurement), while the injection is simulated for a situation far away from equilibrium (representative for an EL measurement).

The differences in the position dependence of $f_i(x)$ and $f_c(x)$ shown in Fig. 4(a) are now translated into an energy dependence of $Q_{e,\mathrm{EL}}$ and $Q_{e,\mathrm{dir}}$ according to Eqs. (10a) and (10b). Depending on the interference pattern in the layer stack that is present for a certain wavelength or photon energy, there will be strong or weak deviations between $Q_{e,\mathrm{EL}}$ and $Q_{e,\mathrm{dir}}$. For instance, if the generation profile leads to high photocurrent generation at the front and very little at the back, the high injection efficiency at the front in Fig. 4(a) will lead to a higher real quantum efficiency as compared to what the more homogenous profile of $f_c$ would cause. If the interferences are such that higher generation rates are observed at the back contact, the low $f_i$ at the back in Fig. 4(a) would lead to the opposite effect. Because the interference pattern will change continuously with wavelength, the ratio $Q_{e,\mathrm{dir}}/Q_{e,\mathrm{EL}}$ will depend on wavelength or photon energy. Of course, the exact interference pattern will depend on the details of the device stack used and on the thicknesses and complex

refractive indices of all layers. Thus, all simulations shown in the following and also in the Supplemental Material [72] are examples that are meant to explain the concept and give an idea of the approximate size of the effect.

Figure 4(b) shows how far the ratio $Q_{e,\mathrm{dir}}/Q_{e,\mathrm{EL}}$ can deviate from a constant (energy independent) for four representative situations keeping the absorber thickness at 200 nm. We simulate the ratio $Q_{e,\mathrm{dir}}/Q_{e,\mathrm{EL}}$ for two cases of asymmetric mobilities ($\mu_n = 10\mu_p = 10^{-3}\ \mathrm{cm^2/V\,s}$ and $\mu_p = 10\mu_n = 10^{-3}\ \mathrm{cm^2/V\,s}$), for symmetric mobilities ($\mu_n = \mu_p = 10^{-3}\ \mathrm{cm^2/V\,s}$) as well as for the case of doping (acceptor density $N_A = 10^{17}\ \mathrm{cm^{-3}}$). In the case of doping, the doping creates a spatially inhomogeneous electric field with a space-charge region towards the cathode and field-free region towards the anode. This leads to spatially inhomogeneous injection and extraction efficiencies that have slightly different position dependencies and cause the ratio $Q_{e,\mathrm{dir}}/Q_{e,\mathrm{EL}}$ to deviate from a constant. The deviations by themselves are rather small given that the quantum efficiencies will change by several orders of magnitude over the energy range where $Q_{e,\mathrm{dir}}$ and $Q_{e,\mathrm{EL}}$ can be compared experimentally. For the case of asymmetric mobilities, however, the ratio $Q_{e,\mathrm{dir}}/Q_{e,\mathrm{EL}}$ can vary substantially because of the spatially inhomogeneous injection efficiency and emission probability. In order to provide an estimate of the maximum deviation between the minimum and maximum value of the ratio $Q_{e,\mathrm{dir}}/Q_{e,\mathrm{EL}}$, we make a series of simulations for various mobility ratios and thicknesses [72]. Based on these results, thicknesses of less than 150 nm and mobility ratios less than 10 should lead to errors of less than 20%, while for higher mobility ratios and thicknesses the error could quickly become substantial. In addition, we study the effect of varying the contact barrier in the presence of asymmetric mobilities as shown in the Supplemental Material, Fig. S8 [72]. From these simulations we see that lower contact barriers lead to slightly higher deviations between the minimum and maximum value of the ratio $Q_{e,\mathrm{dir}}/Q_{e,\mathrm{EL}}$. This is because lower barriers lead to more charge injection into the active layer in the dark and therefore amplify the effect of asymmetric mobilities to lead to spatially inhomogeneous injection efficiencies. Thus, we conclude that under normal circumstances of thin devices with not too asymmetric mobilities, the invalidity of the Donolato theorem has a minor influence on the ratio $Q_{e,\mathrm{dir}}/Q_{e,\mathrm{EL}}$. While deviations would be expected for larger thicknesses and asymmetric mobilities, those can be easily avoided by an appropriate choice of device thickness. This implies that the method as proposed by Vandewal *et al.* [17] should not be affected by a potential invalidity of the Donolato theorem if large thicknesses and asymmetric mobilities are avoided.

## IV. CONCLUSION

In summary, we have studied the effect of nonlinear recombination, space charge, and low mobilities on the validity of two optoelectronic reciprocity relations used to analyze EL spectra and EL intensity in organic solar cells. The two reciprocity relations connect different physical quantities of diodes operated as solar cells with quantities of diodes operated as LEDs, namely, the solar-cell quantum efficiency with the shape of the EL spectrum and the open-circuit voltage with the LED quantum efficiency. Both relations work only if electrical injection from a junction into a semiconductor can be quantitatively related to charge-carrier extraction from the same semiconductor to the junction under illumination (the so-called Donolato theorem). When the open-circuit voltage is related to the LED quantum efficiency, the effect of nonlinear recombination can affect the result. However, we show that the result is affected substantially only at relatively low mobilities and fill factors, meaning that for state-of-the-art organic solar cells, the relation should be applicable. The relation between solar-cell quantum efficiency and EL spectrum can be used to exclude hot-carrier effects in charge generation at the donor:acceptor interface of bulk-heterojunction solar cells. If nonlinear recombination is combined with space-charge effects, i.e., due to asymmetric mobilities, then the shape of the EL spectrum is no longer directly related to the shape of the solar-cell quantum efficiency and the analysis of hot-carrier effects would be impossible or at least error prone. However, space-charge effects can be minimized by reducing cell thickness and we find that in particular for active layer thicknesses around 100 nm the method should be hardly affected by violations of the Donolato theorem.

## ACKNOWLEDGMENTS

T. K. acknowledges support by an Imperial College Junior Research Fellowship, support from the DFG (Grant No. KI-1571/2-1), and from the Helmholtz Association via the Helmholtz Energy Alliance Hybrid PV. In addition, T. K. would like to thank Steve Hawks (UCLA) for stimulating discussions. J. N. acknowledges the Royal Society for a Wolfson Merit Award, and the Engineering and Physical Sciences Research Council for support via Grants No. EP/K030671/1, No. EP/G031088/1, and No. EP/J017361/1.

[1] K. Tvingstedt, K. Vandewal, A. Gadisa, F. L. Zhang, J. Manca, and O. Inganas, Electroluminescence from charge transfer states in polymer solar cells, J. Am. Chem. Soc. **131**, 11819 (2009).

[2] K. Vandewal, K. Tvingstedt, A. Gadisa, O. Inganas, and J. V. Manca, On the origin of the open-circuit voltage of polymer-fullerene solar cells, Nat. Mater. **8**, 904 (2009).

[3] M. A. Faist, T. Kirchartz, W. Gong, R. S. Ashraf, I. McCulloch, J. C. de Mello, N. J. Ekins-Daukes, D. D. C. Bradley, and J. Nelson, Competition between the charge transfer state and the singlet states of donor or acceptor

limiting the efficiency in polymer:fullerene solar cells, J. Am. Chem. Soc. **134**, 685 (2012).

[4] K. Vandewal, Z. Ma, J. Bergqvist, Z. Tang, E. Wang, P. Henriksson, K. Tvingstedt, M. R. Andersson, F. Zhang, and O. Inganas, Quantification of quantum efficiency and energy losses in low bandgap polymer:fullerene solar cells with high open-circuit voltage, Adv. Energy Mater. **22**, 3480 (2012).

[5] S. A. Hawks, F. Deledalle, J. Yao, D. G. Rebois, G. Li, J. Nelson, Y. Yang, T. Kirchartz, and J. R. Durrant, Relating recombination, density of states, and device performance in an efficient polymer:fullerene organic solar cell blend, Adv. Energy Mater. **3**, 1201 (2013).

[6] N. Bansal, L. X. Reynolds, A. MacLachlan, T. Lutz, R. S. Ashraf, W. Zhang, C. B. Nielsen, I. McCulloch, D. G. Rebois, T. Kirchartz, M. S. Hill, K. C. Molloy, J. Nelson, and S. A. Haque, Influence of crystallinity and energetics on charge separation in polymer–inorganic nanocomposite films for solar cells, Sci. Rep. **3**, 1531 (2013).

[7] E. T. Hoke, K. Vandewal, J. A. Bartelt, W. R. Mateker, J. D. Douglas, R. Noriega, K. R. Graham, J. M. J. Frechet, A. Salleo, and M. D. McGehee, Recombination in polymer: fullerene solar cells with open-circuit voltages approaching and exceeding 1.0 V, Adv. Energy Mater. **3**, 220 (2013).

[8] D. di Nuzzo, G. J. A. H. Wetzelaer, R. K. M. Bower, V. S. Gevaerts, S. C. J. Meskers, J. C. Hummelen, P. W. M. Blom, and R. A. J. Janssen, Simultaneous open-circuit voltage enhancement and short-circuit current loss in polymer: Fullerene solar cells correlated by reduced quantum efficiency for photoinduced electron transfer, Adv. Energy Mater. **3**, 85 (2013).

[9] C. W. Schlenker, K. S. Chen, H. L. Yip, C. Z. Li, L. R. Bradshaw, S. T. Ochsenbein, F. Z. Ding, X. S. S. Li, D. R. Gamelin, A. K. Y. Jen, and D. S. Ginger, Polymer triplet energy levels need not limit photocurrent collection in organic solar cells, J. Am. Chem. Soc. **134**, 19661 (2012).

[10] U. Hoyer, M. Wagner, T. Swonke, J. Bachmann, R. Auer, A. Osvet, and C. J. Brabec, Electroluminescence imaging of organic photovoltaic modules, Appl. Phys. Lett. **97**, 233303 (2010).

[11] U. Hoyer, L. Pinna, T. Swonke, R. Auer, C. J. Brabec, T. Stubhan, and N. Li, Comparison of electroluminescence intensity and photocurrent of polymer based solar cells, Adv. Energy Mater. **1**, 1097 (2011).

[12] A. Helbig, T. Kirchartz, R. Schaeffler, J. H. Werner, and U. Rau, Quantitative electroluminescence analysis of resistive losses in Cu(In, Ga)$Se_2$ thin-film modules, Sol. Energy Mater. Sol. Cells **94**, 979 (2010).

[13] M. Seeland, R. Rosch, and H. Hoppe, Quantitative analysis of electroluminescence images from polymer solar cells, J. Appl. Phys. **111**, 024505 (2012).

[14] T. M. H. Tran, B. E. Pieters, C. Ulbrich, A. Gerber, T. Kirchartz, and U. Rau, Transient phenomena in Cu(In, Ga)$Se_2$ solar modules investigated by electroluminescence imaging, Thin Solid Films **535**, 307 (2013).

[15] M. Seeland, R. Rosch, and H. Hoppe, Luminescence imaging of polymer solar cells: Visualization of progressing degradation, J. Appl. Phys. **109**, 064513 (2011).

[16] D. Baran, N. Li, A.-C. Breton, A. Osvet, T. Ameri, M. Leclerc, and C. J. Brabec, Qualitative analysis of bulk-heterojunction solar cells without device fabrication: an elegant and contactless method, J. Am. Chem. Soc. **136**, 10949 (2014).

[17] K. Vandewal, S. Albrecht, E. T. Hoke, K. R. Graham, J. Widmer, J. D. Douglas, M. Schubert, W. R. Mateker, J. T. Bloking, G. F. Burkhard, A. Sellinger, J. M. J. Frechet, A. Amassian, M. K. Riede, M. D. McGehee, D. Neher, and A. Salleo, Efficient charge generation by relaxed charge-transfer states at organic interfaces, Nat. Mater. **13**, 63 (2014).

[18] D. Baran, M. S. Vezie, N. Gasparini, F. Deledalle, J. Yao, B. C. Schroeder, H. Bronstein, T. Ameri, T. Kirchartz, I. McCulloch, J. Nelson, and C. J. Brabec, Role of polymer fractionation in energetic losses and charge carrier lifetimes of polymer: Fullerene solar cells, J. Phys. Chem. C **119**, 19668 (2015).

[19] W. Tress, N. Marinova, O. Inganas, M. K. Nazeeruddin, S. M. Zakeeruddin, and M. Graetzel, Predicting the open-circuit voltage of $CH_3NH_3PBI_3$ perovskite solar cells using electroluminescence and photovoltaic quantum efficiency spectra: The role of radiative and non-radiative recombination, Adv. Energy Mater. **5**, 1400812 (2015).

[20] K. Tvingstedt, O. Malinkiewicz, A. Baumann, C. Deibel, H. J. Snaith, V. Dyakonov, and H. J. Bolink, Radiative efficiency of lead iodide based perovskite solar cells, Sci. Rep. **4**, 6071 (2014).

[21] J. Z. Yao, T. Kirchartz, M. S. Vezie, M. A. Faist, W. Gong, Z. C. He, H. B. Wu, J. Troughton, T. Watson, D. Bryant, and J. Nelson, Quantifying Losses in Open-Circuit Voltage in Solution-Processable Solar Cells, Phys. Rev. Applied **4**, 014020 (2015).

[22] U. Rau, Reciprocity relation between photovoltaic quantum efficiency and electroluminescent emission of solar cells, Phys. Rev. B **76**, 085303 (2007).

[23] U. Rau, Superposition and reciprocity in the electroluminescence and photoluminescence of solar cells, IEEE J. Photovoltaics **2**, 169 (2012).

[24] U. Rau and R. Brendel, The detailed balance principle and the reciprocity theorem between photocarrier collection and dark carrier distribution in solar cells, J. Appl. Phys. **84**, 6412 (1998).

[25] T. Kirchartz and U. Rau, Detailed balance and reciprocity in solar cells, Phys. Status Solidi A **205**, 2737 (2008).

[26] P. W. Bridgman, Note on the principle of detailed balancing, Phys. Rev. **31**, 101 (1928).

[27] B. E. Pieters, T. Kirchartz, T. Merdzhanova, and R. Carius, Modeling of photoluminescence spectra and quasi-Fermi level splitting in mu *c*-Si:H solar cells, Sol. Energy Mater. Sol. Cells **94**, 1851 (2010).

[28] W. Gong, M. A. Faist, N. J. Ekins-Daukes, Z. Xu, D. D. C. Bradley, J. Nelson, and T. Kirchartz, Influence of energetic disorder on electroluminescence emission in polymer:fullerene solar cells, Phys. Rev. B **86**, 024201 (2012).

[29] T. Kirchartz, T. Agostinelli, M. Campoy-Quiles, W. Gong, and J. Nelson, Understanding the thickness-dependent performance of organic bulk heterojunction solar cells: The influence of mobility, lifetime and space charge, J. Phys. Chem. Lett. **3**, 3470 (2012).

[30] C. G. Shuttle, B. O'Regan, A. M. Ballantyne, J. Nelson, D. D. C. Bradley, J. de Mello, and J. R. Durrant, Experimental

determination of the rate law for charge carrier decay in a polythiophene: Fullerene solar cell, Appl. Phys. Lett. **92**, 093311 (2008).

[31] C. G. Shuttle, R. Hamilton, B. C. O'Regan, J. Nelson, and J. R. Durrant, Charge-density-based analysis of the current-voltage response of polythiophene/fullerene photovoltaic devices, Proc. Natl. Acad. Sci. U.S.A. **107**, 16448 (2010).

[32] C. G. Shuttle, A. Maurano, R. Hamilton, B. O'Regan, J. C. de Mello, and J. R. Durrant, Charge extraction analysis of charge carrier densities in a polythiophene/fullerene solar cell: Analysis of the origin of the device dark current, Appl. Phys. Lett. **93**, 183501 (2008).

[33] F. A. Lindholm, J. G. Fossum, and E. L. Burgess, Application of the superposition principle to solar-cell analysis, IEEE Trans. Electron Devices **26**, 165 (1979).

[34] X. F. Wang and M. S. Lundstrom, On the use of Rau's reciprocity to deduce external radiative efficiency in solar cells, IEEE J. Photovoltaics **3**, 1348 (2013).

[35] T. Kirchartz, J. Bisquert, I. Mora-Sero, and G. Garcia-Belmonte, Classification of solar cells according to mechanisms of charge separation and charge collection, Phys. Chem. Chem. Phys. **17**, 4007 (2015).

[36] T. Kirchartz, A. Helbig, W. Reetz, M. Reuter, J. H. Werner, and U. Rau, Reciprocity between electroluminescence and quantum efficiency used for the characterization of silicon solar cells, Prog. Photovoltaics **17**, 394 (2009).

[37] K. Vandewal, K. Tvingstedt, A. Gadisa, O. Inganas, and J. V. Manca, Relating the open-circuit voltage to interface molecular properties of donor:acceptor bulk heterojunction solar cells, Phys. Rev. B **81**, 125204 (2010).

[38] A. E. Jailaubekov, A. P. Willard, J. R. Tritsch, W. L. Chan, N. Sai, R. Gearba, L. G. Kaake, K. J. Williams, K. Leung, P. J. Rossky, and X. Y. Zhu, Hot charge-transfer excitons set the time limit for charge separation at donor/acceptor interfaces in organic photovoltaics, Nat. Mater. **12**, 66 (2013).

[39] S. D. Dimitrov, A. A. Bakulin, C. B. Nielsen, B. C. Schroeder, J. P. Du, H. Bronstein, I. McCulloch, R. H. Friend, and J. R. Durrant, On the energetic dependence of charge separation in low-band-gap polymer/fullerene blends, J. Am. Chem. Soc. **134**, 18189 (2012).

[40] G. Grancini, M. Maiuri, D. Fazzi, A. Petrozza, H. J. Egelhaaf, D. Brida, G. Cerullo, and G. Lanzani, Hot exciton dissociation in polymer solar cells, Nat. Mater. **12**, 29 (2013).

[41] G. Grancini, M. Binda, L. Criante, S. Perissinotto, M. Maiuri, D. Fazzi, A. Petrozza, H. J. Egelhaaf, D. Brida, G. Cerullo, and G. Lanzani, Measuring internal quantum efficiency to demonstrate hot exciton dissociation Reply, Nat. Mater. **12**, 594 (2013).

[42] A. Armin, Y. L. Zhang, P. L. Burn, P. Meredith, and A. Pivrikas, Measuring internal quantum efficiency to demonstrate hot exciton dissociation, Nat. Mater. **12**, 593 (2013).

[43] M. Scharber, Measuring internal quantum efficiency to demonstrate hot exciton dissociation, Nat. Mater. **12**, 594 (2013).

[44] C. Silva, Organic photovoltaics: Some like it hot, Nat. Mater. **12**, 5 (2013).

[45] A. A. Bakulin, A. Rao, V. G. Pavelyev, P. H. M. van Loosdrecht, M. S. Pshenichnikov, D. Niedzialek, J. Cornil, D. Beljonne, and R. H. Friend, The role of driving energy and delocalized states for charge separation in organic semiconductors, Science **335**, 1340 (2012).

[46] R. T. Ross, Some thermodynamics of photochemical systems, J. Chem. Phys. **46**, 4590 (1967).

[47] G. Smestad and H. Ries, Luminescence and current voltage characteristics of solar-cells and optoelectronic devices, Sol. Energy Mater. Sol. Cells **25**, 51 (1992).

[48] C. Donolato, An alternative proof of the generalized reciprocity theorem for charge collection, J. Appl. Phys. **66**, 4524 (1989).

[49] C. Donolato, A reciprocity theorem for charge collection, Appl. Phys. Lett. **46**, 270 (1985).

[50] M. A. Green, Generalized relationship between dark carrier distribution and photocarrier collection in solar cells, J. Appl. Phys. **81**, 268 (1997).

[51] T. Markvart, Relationship between bark carrier distribution and photogenerated carrier collection in solar cells, IEEE Trans. Electron Devices **43**, 1034 (1996).

[52] K. Misiakos and F. A. Lindholm, Generalized reciprocity theorem for semiconductor-devices, J. Appl. Phys. **58**, 4743 (1985).

[53] T. Markvart, Thermodynamics of losses in photovoltaic conversion, Appl. Phys. Lett. **91**, 064102 (2007).

[54] T. Markvart, Solar cell as a heat engine: Energy-entropy analysis of photovoltaic conversion, Phys. Status Solidi A **205**, 2752 (2008).

[55] U. Rau, U. W. Paetzold, and T. Kirchartz, Thermodynamics of light management in photovoltaic devices, Phys. Rev. B **90**, 035211 (2014).

[56] P. Würfel, T. Trupke, T. Puzzer, E. Schaffer, W. Warta, and S. W. Glunz, Diffusion lengths of silicon solar cells from luminescence images, J. Appl. Phys. **101**, 123110 (2007).

[57] D. Hinken, K. Bothe, K. Ramspeck, S. Herlufsen, and R. Brendel, Determination of the effective diffusion length of silicon solar cells from photoluminescence, J. Appl. Phys. **105**, 104516 (2009).

[58] L. Goris, A. Poruba, L. Hod'akova, M. Vanecek, K. Haenen, M. Nesladek, P. Wagner, D. Vanderzande, L. De Schepper, and J. V. Manca, Observation of the subgap optical absorption in polymer-fullerene blend solar cells, Appl. Phys. Lett. **88**, 052113 (2006).

[59] J. Lee, K. Vandewal, S. R. Yost, M. E. Bahlke, L. Goris, M. A. Baldo, J. V. Manca, and T. Van Voorhis, Charge transfer state versus hot exciton dissociation in polymer-fullerene blended solar cells, J. Am. Chem. Soc. **132**, 11878 (2010).

[60] R. A. Street, K. W. Song, J. E. Northrup, and S. Cowan, Photoconductivity measurements of the electronic structure of organic solar cells, Phys. Rev. B **83**, 165207 (2011).

[61] R. A. Street, A. Krakaris, and S. R. Cowan, Recombination through different types of localized states in organic solar cells, Adv. Funct. Mater. **22**, 4608 (2012).

[62] Z. E. Ooi, R. Jin, J. Huang, Y. F. Loo, A. Sellinger, and J. C. deMello, On the pseudo-symmetric current-voltage response of bulk heterojunction solar cells, J. Mater. Chem. **18**, 1644 (2008).

[63] G. F. A. Dibb, T. Kirchartz, D. Credgington, J. R. Durrant, and J. Nelson, Analysis of the relationship between linearity

of corrected photocurrent and the order of recombination in organic solar cells, J. Phys. Chem. Lett. **2**, 2407 (2011).

[64] A. Petersen, T. Kirchartz, and T. A. Wagner, Charge extraction and photocurrent in organic bulk heterojunction solar cells, Phys. Rev. B **85**, 045208 (2012).

[65] M. Limpinsel, A. Wagenpfahl, M. Mingebach, C. Deibel, and V. Dyakonov, Photocurrent in bulk heterojunction solar cells, Phys. Rev. B **81**, 085203 (2010).

[66] D. J. Wehenkel, L. J. A. Koster, M. M. Wienk, and R. A. J. Janssen, Influence of injected charge carriers on photocurrents in polymer solar cells, Phys. Rev. B **85**, 125203 (2012).

[67] See Supplemental Material at http://link.aps.org/supplemental/10.1103/PhysRevApplied.5.054003, Sec. A, for the derivation of Eq. (7).

[68] B. E. Pieters, J. Krc, and M. Zeman, in *Conference Record of the 2006 IEEE 4th World Conference on Photovoltaic Energy Conversion* (IEEE, New York, 2006), p. 1513.

[69] T. Kirchartz, B. E. Pieters, J. Kirkpatrick, U. Rau, and J. Nelson, Recombination via tail states in polythiophene: Fullerene solar cells, Phys. Rev. B **83**, 115209 (2011).

[70] See Supplemental Material at http://link.aps.org/supplemental/10.1103/PhysRevApplied.5.054003, Sec. B, for additional simulations on the error in predicted open-circuit voltage relative to the recombination loss at short circuit.

[71] See Supplemental Material at http://link.aps.org/supplemental/10.1103/PhysRevApplied.5.054003, Sec. C, for the differences between collection and injection efficiencies at different thicknesses and the consequent changes in the ratio $Q_{e,\mathrm{dir}}/Q_{e,\mathrm{EL}}$.

[72] See Supplemental Material at http://link.aps.org/supplemental/10.1103/PhysRevApplied.5.054003, Sec. D, for various simulations with asymmetric mobilities, different thicknesses, and different contact barriers.